The Journal of Chemical Physics

Interfacial free energy of a liquid-solid interface: Its change with curvature

Cite as: J. Chem. Phys. **151**, 144501 (2019); https://doi.org/10.1063/1.5121026
Submitted: 22 July 2019 . Accepted: 16 September 2019 . Published Online: 08 October 2019

P. Montero de Hijes, Jorge R. Espinosa, Eduardo Sanz, and Carlos Vega

J. Chem. Phys. **151**, 144501 (2019); https://doi.org/10.1063/1.5121026

AIP Publishing

The Journal of Chemical Physics | ARTICLE | scitation.org/journal/jcp

Interfacial free energy of a liquid-solid interface: Its change with curvature

Cite as: J. Chem. Phys. 151, 144501 (2019); doi: 10.1063/1.5121026
Submitted: 22 July 2019 • Accepted: 16 September 2019 •
Published Online: 8 October 2019

View Online Export Citation CrossMark

P. Montero de Hijes,[1] Jorge R. Espinosa,[2,3] Eduardo Sanz,[1] and Carlos Vega[1,a)]

AFFILIATIONS

[1] Departamento de Química Física, Facultad de Ciencias Químicas, Universidad Complutense de Madrid, 28040 Madrid, Spain
[2] Maxwell Centre, Cavendish Laboratory, Department of Physics, University of Cambridge, Cambridge CB3 0H3, United Kingdom
[3] Emmanuel College, Cambridge CB2 3AP, United Kingdom

[a)] **Electronic mail:** cvega@quim.ucm.es

ABSTRACT

We analyze the changes in the interfacial free energy between a spherical solid cluster and a fluid due to the change of the radius of the solid. Interfacial free energies from nucleation studies using the seeding technique for four different systems, being hard spheres, Lennard-Jones, and two models of water (mW and TIP4P/ICE), were plotted as a function of the inverse of the radius of the solid cluster. In all cases, the interfacial free energy was a linear function of the inverse of the radius of the solid cluster and this is consistent with Tolman's equation. This linear behavior is shown not only in isotherms but also along isobars. The effect of curvature on the interfacial free energy is more pronounced in water, followed by hard spheres, and smaller for Lennard-Jones particles. We show that it is possible to estimate nucleation rates of Lennard-Jones particles at different pressures by using information from simple NpT simulations and taking into account the variation of the interfacial free energy with the radius of the solid cluster. Neglecting the effects of the radius on the interfacial free energy (capillarity approximation) leads to incorrect values of the nucleation rate. For the Lennard-Jones system, the homogeneous nucleation curve is not parallel to the melting curve as was found for water in previous work. This is due to the increase in the interfacial free energy along the coexistence curve as the pressure increases. This work presents a simple and relatively straightforward way to approximately estimate nucleation rates.

I. INTRODUCTION

When there is an interface between two phases, there is a contribution to the free energy that can be assigned to the presence of such an interface. When given per unit of area, this defines the interfacial free energy γ. Strictly speaking, γ is a well and uniquely defined property, in the thermodynamic sense, when the interface between the two phases is planar so that the interfacial area is a well-defined property and when the chemical potential of the two phases is identical. Only in this way can one obtain the interfacial contribution in a nonambiguous way. Thus, the value of γ has been extensively reported in experiments where one studies the vapor-liquid equilibrium at coexistence conditions with a planar interface.[1,2] When any of these two conditions is not satisfied (either the interface is not planar or the chemical potential of both phases in the bulk is not the same), then it is not possible to define uniquely γ and the value obtained will depend on a certain arbitrary choice.[2–4] Such a choice defines where one of the phases finishes and where the other phase begins (through a dividing surface in the traditional description or through an order parameter as in more modern simulation studies). Even acknowledging this limitation, one could still recognize that it may be possible to make a specific choice that leads to a value of γ that is useful from a practical point of view. A particular area in which having a value of γ could be useful is homogeneous crystal nucleation, which in turn plays a central role in a broad range of disciplines such as climate science,[5] food industry,[6] or material science,[7] to mention just a few.

In the last 20 years, molecular simulation studies have led to huge progress in our understanding of the nucleation of solid phases. Nowadays, techniques such as forward flux sampling (FFS)[8] and/or transition path sampling (TPS)[9] allow us to compute the nucleation rate J (i.e., number of critical solid clusters per unit of volume and time) in a rigorous way. Another approach to J was a combination of the traditional formalism of Volmer-Weber[10]-Becker-Doring[11] (VWBD) and computer simulations.[1,12] This pioneering route was first used by Auer and Frenkel[13,14] and followed by others.[15–18] Hence, the key equation leading to J is

$$J = \rho_{liq}\sqrt{(|\Delta G''|_{N_c}/(2\pi kT))}f^{+}\exp(-\Delta G_c/(kT)). \tag{1}$$

All that is needed in Eq. (1) can be obtained from computer simulations: the density of the liquid ρ_{liq}, the attachment rate f^{+}, the free energy barrier to nucleation ΔG_c, and the Zeldovich factor $Z = \sqrt{(|\Delta G''|_{N_c}/(2\pi kT))}$, where $|\Delta G''|_{N_c}$ is the second derivative of the Gibbs free energy of the system with respect to the size of the solid cluster (evaluated at the critical particle size N_c). Typically, the values of Z and ΔG_c are obtained using the well-known biasing technique umbrella sampling (US),[19] which commonly gives name to the whole procedure of Auer and Frenkel, although they can also be obtained via metadynamics.[20,21] In a very important paper, Filion *et al.*[15] showed that US leads to values of J practically identical to those obtained from FFS. Filion *et al.* not only showed that the values of J agree very well with those obtained from other routes, but they also showed that the free energy barrier (and the product Zf^{+}) did not depend significantly on the order parameter chosen to label the molecules as liquid or solid. A similar conclusion was recently reached by Prestipino[17] for the Lennard-Jones (LJ) and water mW[22] models. Consequently, the obtained values of J were not sensitive to the choice of the order parameter. Note that the value of γ is not used/needed when estimating J by means of US.

As computational studies for J (either using US, FFS, or TPS) are rather expensive, in recent years, we have proposed a somewhat different version of Eq. (1) that was denoted as seeding.[23–29] In this technique,[25–28] a cluster of the solid phase is inserted into the metastable liquid and the thermodynamic conditions are varied until the cluster becomes critical (i.e., going to the liquid phase half of the times and to the solid phase the other half). Then, the value of J is estimated as

$$J = \rho_{liq}\sqrt{\frac{|\Delta\mu|}{6\pi kTN_c}}f^{+}\exp[(-\Delta\mu N_c)/(2kT)], \tag{2}$$

where $\Delta\mu$ is the difference in chemical potential between the bulk liquid and the bulk solid at the considered conditions of temperature T and pressure p. The main difference with Eq. (1) is that, instead of computing Z and ΔG_c rigorously, they are now estimated from the well-known equations of Classical Nucleation Theory (CNT).[1,30] While Eq. (1) is almost exact and leads to practically exact values of J, Eq. (2) is not, and hence, leads to approximate values of J. The reason why results from Eq. (2) are approximate is that they depend dramatically on the selection of the order parameter chosen to define the number of particles N_c in the critical cluster of radius R_c. The impact of that choice on the value of J has been discussed in detail recently by some of the authors.[31] However, we have found over the last few years that a sensible choice of the order parameter (used to label the molecules as liquid and solid) using the methodology of Lechner and Dellago[32] along with the so-called mislabeling criterium[28,33,34] leads to quite reasonable estimates of J for the following systems: hard spheres, LJ, NaCl, and several water models. One can summarize the situation by saying that for a certain choice of the order parameter, the combination of the VWBD formalism and the CNT yields very good predictions of the nucleation rate J, which is an experimentally accessible property. We shall denote Eq. (2) as seeding which can be regarded as a combination of the VWBD formalism and Classical Nucleation Theory with input obtained from computer simulations. Besides, CNT relates the interfacial free energy and the size of the critical cluster,

$$\gamma_{CNT} = \left(\frac{3N_c\rho_{sol}^2|\Delta\mu|^3}{32\pi}\right)^{1/3}, \tag{3}$$

where ρ_{sol} is the density of the solid. One should keep in mind that γ_{CNT} is not unique as it depends on the selection of the order parameter so it is not possible to define interfacial free energies in a unique way when the interface is not planar (and/or the chemical potentials of the two bulk phases are not identical). However, there is a certain choice of the order parameter that yields a value of γ_{CNT} that allows one to correctly estimate the free energy barrier to nucleation ΔG_c as

$$\Delta G_c = \frac{16\pi\gamma_{CNT}^3}{3\rho_s^2|\Delta\mu|^2}. \tag{4}$$

Note that Eqs. (3) and (4) both assume a spherical shape for the critical cluster. We have shown in the past[28] that a judicious choice of the order parameter combined with the seeding technique leads to the values of N_c and γ_{CNT} that allows one to obtain reasonable estimates of ΔG_c and J. Thus, we can conclude that an order parameter based on the mislabeling criterion is able to produce values of γ_{CNT}, which makes the CNT formalism (in combination with the VWBD kinetic formalism) a useful approach to study nucleation problems.

II. INTERFACIAL FREE ENERGY

In 1949, Tolman suggested that the value of γ of a spherical interface is different from that of a planar interface.[35] Still the best source to read about this issue is the classic book of Rowlinson and Widom, and we refer the reader to this Ref. 2. The variation of γ with the radius of the interface is given by Tolman's equation,

$$\gamma = \gamma_0\left(1 - \frac{2\delta_{Tolman}}{R}\right). \tag{5}$$

Here, R is the radius of the phase forming the sphere (a solid phase in this paper), δ_{Tolman} is a constant, and γ_0 is the interfacial free energy of the planar interface at coexistence. Tolman's equation was derived to describe the variation of γ with the radius of the spherical phase while keeping the temperature constant. To derive the previous equation, Tolman introduced a number of approximations that are described in the original paper (i.e., neglecting terms to evaluate an integral and performing a Taylor expansion over the final result), but more importantly, it was assumed that the distance between the equimolar surface and the surface of tension (that for which Laplace's equation is valid) was constant and did not depend on the radius of the spherical phase. Thus, according to Tolman, the parameter δ_{Tolman} is just the distance between the equimolar dividing surface and the surface of tension, and for this reason, it is usually denoted as the Tolman length. However, there is another simple way of looking at Eq. (5). For the planar interface, the radius of curvature is infinite and Tolman's equation can be regarded as a simple Taylor expansion of γ in powers of $1/R$ truncated at first order. Of course, that means that second and higher order terms are neglected. Whether these terms are important or not can be tested by plotting γ as a function of $1/R$ and looking for deviations from linearity. Another important consideration is that the value of γ in Eq. (5) refers to that at the surface of tension and so R corresponds to such surface (thus, $\gamma = \gamma_s$ and $R = R_s$). This is a convenient choice because, in nucleation studies, it is the surface of tension the dividing surface considered[30,36,37] and, for this reason, $\gamma_s \simeq \gamma_{CNT}$ and $R_s \simeq R_c$. Tolman's equation and the Tolman length have been the focus of many studies, and still it is a matter of intense debate.[36,38–53]

In our previous work, by using the seeding technique, we have obtained the values of γ_{CNT} for the liquid-solid interface.[28,54] Here, we shall analyze in more detail whether the obtained values of γ_{CNT} when plotted as a function of $1/R_c$ are linear or not. There is a subtle issue though concerning the value of the interfacial free energy for the planar interface at equilibrium γ_0 (i.e., at a certain point of the coexistence curve between the liquid and the solid). Let us assume that we want to study the nucleation of a solid at a certain (T, p), at which the radius of the critical cluster is R_c. Outside the liquid-solid coexistence curve, the value of the interfacial free energy for a planar interface is not uniquely defined (i.e., it depends on an arbitrary choice of the order parameter). However, at coexistence, the interfacial free energy between two planar interfaces is well defined, unique, and can be measured in an experimental laboratory. For this reason, it is very convenient to have a simple way of mapping from γ_0 to γ as in Eq. (5). There are, at least, two reasonable options when one is interested in the state (T, p). The first one is the coexistence point at the same pressure. The second is the coexistence point at the same temperature (this second choice was the one adopted by Tolman). Strictly speaking, there are many more as there are infinitely many curves connecting a point of the coexistence curve with the state of interest (T, p). This is illustrated in Fig. 1. In panel (a), the liquid-solid coexistence line of the mW model is shown.[55] In panel (b), the liquid-solid[56] and vapor-liquid[57] coexistence lines of the LJ model are shown as solid lines (and their extension in the metastable region as dashed lines). As shown in Fig. 1(a) for the mW model, as the reference of the value of the interfacial free energy of the planar interface, one could choose either the coexistence point at the same T or the coexistence point at the same p. It seems that for studies dealing with the liquid-solid equilibria, the choice of γ_0 at the same pressure is more convenient. For instance, for the Lennard-Jones system [see Fig. 1(b)], for the state on the left hand side, the value of γ_0 at the same T may occur at negative pressures and cavitation of the liquid could prevent its determination. On the other hand, for the vapor-liquid interface, the state on the right hand side, the opposite holds true. In fact, when studying the cavitation of the liquid at slightly negative pressures, γ_0 should be chosen at the same T, as the vapor pressure is always positive and there is no point of the coexistence curve at negative pressures. Therefore, we shall rewrite Eq. (5) as

$$\gamma_{CNT} = \gamma_{0,T}\left(1 - \frac{2\delta_T}{R_c}\right), \tag{6}$$

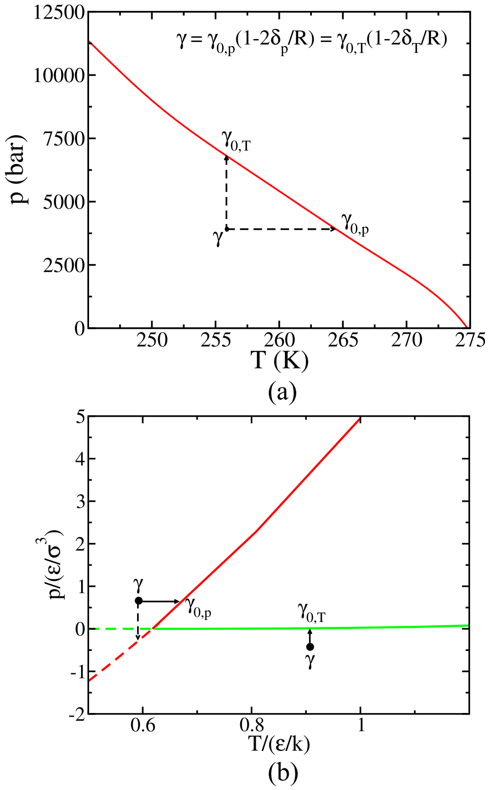

FIG. 1. (a) Schematic representation of a hypothetical γ value with respect to the melting line of the mW water model,[55] and its relation with two different coexistence γ_0 values, one along the isotherm $\gamma_{0,T}$ and one along the isobar $\gamma_{0,p}$. (b) Sketch of the phase diagram of the LJ model (melting[56] and vapor-liquid[57] lines in red and green, respectively) suggesting that for a given problem, one could be more interested in working along isobars than isotherms and vice versa.

$$\gamma_{CNT} = \gamma_{0,p}\left(1 - \frac{2\delta_p}{R_c}\right). \tag{7}$$

Obviously, the value of δ depends on the choice of γ_0. Hence, we shall keep the notation δ_p or δ_T to clarify this. Since all our previous studies of seeding were done at constant pressure, we shall adopt Eq. (7) as our working expression (except for the hard sphere system where the seeding was done at constant temperature and we will use Eq. (6)).

The main idea of this work is to plot all the values of γ_{CNT} obtained in our previous studies of seeding as a function of $1/R_c$ and to analyze the functional dependence that they describe. In particular, whether or not they appear linear. Note that this is a post-analysis of all our previously published results as this aspect was not considered in our anterior work.

For the Lennard-Jones (LJ) system, our preceding study was done only for a pressure close to zero [i.e., $p^* = p/(\epsilon/\sigma^3) = -0.02 \simeq 0$]. Since it would be useful to analyze the effect of pressure for different systems, we include another seeding calculation of the LJ model under a different pressure $p^* = 4.95$. Details on the calculations are similar to those described in our previous work.[28] Note that the LJ

TABLE I. Results from seeding calculations for the LJ system at a reduced pressure of $p^* = p/(\epsilon/\sigma^3) = 4.95$. Number densities for the fluid and solid phase are given in reduced units [i.e., $\rho^* = (N/V)\sigma^3$]. The total number of molecules of the simulation N_T and that of the critical cluster N_c are given and also the reduced temperature at which the cluster is critical. We also report the chemical potential difference between the fluid and the solid $\Delta\mu$, the interfacial free energy per unit of area γ_{CNT}, the attachment rate f^+, the attachment length λ, the free energy barrier for nucleation ΔG_c, and the logarithm of the nucleation rate J. τ is the unit of time in reduced units (i.e., $\tau = \sqrt{m\sigma^2/\epsilon}$).

N_c	N_T	$T/(\epsilon/k)$	ρ^*_{liq}	ρ^*_{sol}	$\lvert\Delta\mu\rvert/(kT)$	$\gamma_{CNT}/(\epsilon/\sigma^2)$	$f^+/(1/\tau)$	λ/σ	$\Delta G_c/(kT)$	$\text{Log}_{10}(J\sigma^3\tau)$
576	31 901	0.854	0.951	1.030	0.215	0.483	862.1	0.59	62	−26
3 810	87 665	0.915	0.940	1.019	0.114	0.512	2802.0	0.68	217	−94
12 678	275 758	0.945	0.934	1.015	0.075	0.518	3448.6	0.97	475	−206

model considered is the truncated and shifted LJ potential in the form proposed by Broughton and Gilmer[58] and described in more detail by Laird *et al.*[56] The results of the seeding calculations are presented in Table I. This allows us to analyze, for LJ and the water models, if the values of δ_p are affected by pressure.

The main result of this work is shown in Fig. 2. Values of γ_{CNT} that are calculated by means of the seeding technique are shown as a function of $1/R_c$, which were obtained along one isotherm for the HS system (using the continuous version of Jover *et al.*[59]) and along several isobars for the rest of the systems. Results are presented for the HS system, for the LJ system[58] (two isobars), for the TIP4P/ICE[60] model of water (two isobars), and for the mW model[22] of water (three isobars).[28,54,61] As can be seen, γ_{CNT} is reasonably well described (within the error estimates) by a linear fit when it is plotted as a function of $1/R_c$. Systematic error sources come from the order parameter choice, while statistical errors may occur due to the stochasticity of the molecular dynamics trajectory. In this case, more trajectories could help minimize uncertainties. In addition, for the smaller critical clusters, the error estimate increases as the preparation is more complicated and the lifetime of the seed decreases since it is more sensitive to fluctuations. In any case, the uncertainties of γ_{CNT} usually happen to be in the range of 3%–7% being somewhat larger for the smaller clusters (i.e., low values of R_c). It should be mentioned that for the interface between a liquid and a solid, the interfacial free energy of a planar interface at coexistence depends on the plane (as given by its Miller indices) of the solid in contact with the liquid.[62–67] The anisotropy is in general small (differences between planes are of about 5%–8%).[68] We have also included in the fit the value of γ for $1/R_c = 0$ estimated as the average for three planes of the interfacial free energy at coexistence (at the same

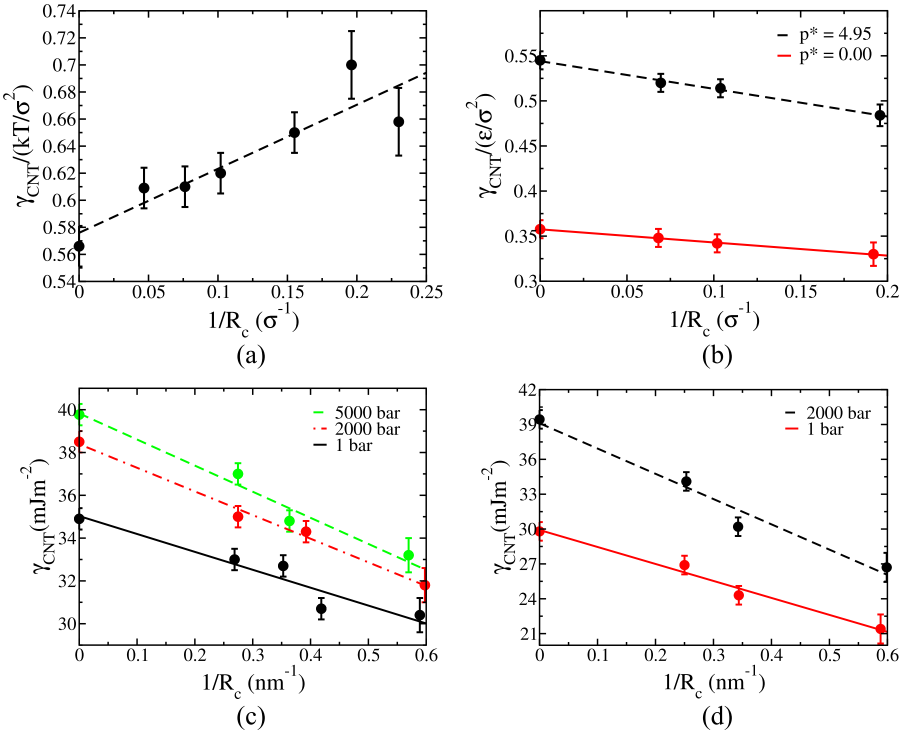

FIG. 2. γ_{CNT} against $1/R_c$ for (a) HS (one isotherm), (b) LJ (two isobars), (c) mW (three isobars), and (d) TIP4P/ICE (two isobars). Error bars for γ_{CNT} are in the range of 3%–7%. The parameters of the expansion analogous to the Tolman lengths are obtained from the linear fits.

pressure for the LJ and water systems). The planes considered were {100}, {110}, and {111} for HS and LJ systems, and basal, primary prismatic and secondary prismatic for water models, respectively. The values of γ_0 obtained from rigorous calculations were taken from previous work.[54,56,62,63,68–71] Note that for $p^* = 4.95$, we have computed, in this work, the interfacial free energy at coexistence $[T/(\epsilon/k) = 1.000]$ by means of the mold integration technique[68] for two crystal orientations {100} and {111}. The obtained values for $\gamma_{0,p}$ were 0.56(1) and 0.51(1), respectively, in good agreement with previous estimations from Laird *et al.* who reported values for three planes at different coexistence conditions.[56] The numerical details for the new calculations are identical as reported for those same crystal orientations at coexistence conditions $p^* = 0.00$ and $T/(\epsilon/k) = 0.618$ in previous work.[68] As discussed in detail by Koß *et al.*,[72,73] the fact that the crystal-fluid interfacial free energy depends on the exposed plane makes very large clusters (i.e., close to coexistence conditions) to become nonspherical and adopt a polyhedric form probably given by the Wulff construction. The surface area of such a polyhedric nucleus is larger than the surface area of a sphere with the same volume. Hence, assuming a spherical shape leads to an overestimated surface free energy. It depends on the considered system size whether these anisotropy effects can be neglected or not. Nevertheless, for the clusters considered in this work (in most cases $N_c < 18\,000$), we observed all of them to be spherical.

As can be seen, the results of this work for the liquid-solid interface can be described by a linear function of $1/R_c$ (although for the vapor-liquid equilibria, it has been suggested that quadratic terms should be included[74,75]). The values of δ_T and $\gamma_{0,T}$ for HS as well as δ_p and $\gamma_{0,p}$ for LJ and the two models of water (mW and TIP4P/ICE) arising from the fits to Eqs. (6) and (7), respectively, are presented in Table II along with their corresponding errors.

For the mW, our seeding results were obtained through isobars. However, we were able to obtain the variation of γ with $1/R_c$ along isotherms by interpolation. As shown in Fig. 3, γ_{CNT} can be well described by a linear function of $1/R_c$ both through isotherms and isobars. The values of δ_T obtained are 0.24, 0.31, and 0.38 (in nm) for T = 240, 250, and 257, 5 (K) respectively, whereas the values of $\gamma_{0,T}$ are 42.75, 42.69, and 41.86 (in mJ/m^2), respectively,. As can be seen from the values of Table II, for the mW model, the values of δ_T are higher (by a factor of about two) than the values of δ_p.

TABLE II. γ_0: Values of the interfacial free energy of the planar interface at coexistence conditions (sub T or p depending on which variable was kept constant) in units of HS (kT/σ^2), LJ (ϵ/σ^2), and water models mW and TIP4P/ICE (mJ/m^2). δ: Values of the expansion coefficient analogous to the Tolman length obtained from a linear fit of γ_{CNT} data in units of HS and LJ (σ) and water models mW and TIP4P/ICE (nm). For the LJ system, the reduced pressure p^* is given in units of ϵ/σ^3. The reported uncertainties include the contribution from the standard error of the fit and the contribution due to the error bars in γ_{CNT}.

	$\gamma_{0,T}$	δ_T
HS	0.576(19)	−0.41(11)
	$\gamma_{0,p}$	δ_p
LJ$_{p^*=0.00}$	0.358(3)	0.203(13)
LJ$_{p^*=4.95}$	0.543(6)	0.286(33)
mW$_{p=1\text{ bar}}$	35.0(8)	0.12(3)
mW$_{p=2000\text{ bars}}$	38.4(5)	0.14(3)
mW$_{p=5000\text{ bars}}$	39.8(7)	0.15(3)
TIP4P/ICE$_{p=1\text{ bar}}$	29.9(9)	0.24(4)
TIP4P/ICE$_{p=2000\text{ bars}}$	39.1(1.4)	0.28(5)

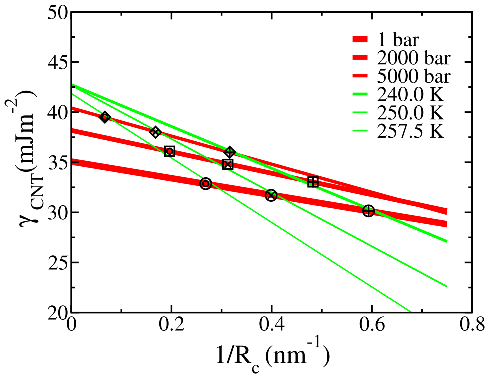

FIG. 3. Fits of isobars (red lines) and isotherms (green lines) of γ_{CNT} vs $1/R_c$ for mW. Symbols correspond to the computed values that are fitted. There are two overlapping symbols for each value indicating which isotherm and isobar are the corresponding ones. Inner symbols imply isotherms, whereas the outer symbols imply isobars. Outer: diamonds (5000 bars), squares (2000 bars), and circles (1 bar). Inner: circles (257.5 K), crosses (250.0 K), and pluses (240 K). Error bars are omitted for clarity, although they are of the same order of magnitude as those of Fig. 2.

In principle, δ_T and δ_{Tolman} should be identical as both correspond to isotherms, and the surface to be considered in nucleation studies is that at which Tolman's equation is referred, which is the surface of tension. For this reason, δ_T in principle should correspond to the distance (difference) between the equimolar radius and the radius at the surface of tension (after assuming that it is constant along the isotherm). Part of the problem when checking this point is that although the equimolar radius is easily obtained from a density profile, the radius of tension can only be determined rigorously by determining the free energy of the system. Since free energy calculations are expensive, little or almost nothing is known about the radius of tension. This has made it difficult to obtain definitive conclusions on this issue for many years. Here, we simply show that γ_{CNT} is well described by a linear expansion over $1/R_c$, pointing out that further studies are required to establish the relation between the slope and the distance between the two surfaces. Besides, when plots are made along isobars, there is no molecular theory explaining the origin of the value of δ_p (see, however, Ref. 49 for a recent approach). In any case, from a practical point of view, it is enough to know that the dependence of γ_{CNT} with $1/R_c$ is well described by a linear curve.

From the results of Table II, it can be concluded that the values of δ_T and δ_p are smaller than a molecular diameter. In terms of the molecular diameter, they were found to be of about 1/4 for the LJ, 4/10 for the HS and the mW model of water, and of about 9/10 for the TIP4P/ICE model of water (the molecular diameter of water is typically of about 0.31 nm, and the first peak of the oxygen-oxygen correlation function is located around 0.28 nm). This also means that the impact of curvature effects on γ decreases in the order: water (TIP4P/ICE), water(mW), HS, and LJ.

It should be recognized that when describing the values of γ_{CNT} by using Eqs. (6) and (7) both the impact of curvature and of the thermodynamic driving force are incorporated into the fit (i.e., when changing the size of the critical cluster one is also changing the value of $\Delta\mu$). We believe that this is a useful approach from a practical point of view as the value of the interfacial free energy of a planar interface cannot be defined uniquely when the system is not at the equilibrium conditions.[3,4] Attempts have been made to evaluate the impact of curvature at constant thermodynamic conditions.[44] Here, our approach is to include both effects (curvature and driving force) into the description as, in our view, the impact of curvature and thermodynamic driving force cannot be determined separately in a nonambiguous way.

Another key issue is the sign of δ. For the HS, δ_T is negative. For the rest of the systems, δ_p is positive. We also found that for the mW, δ_T was positive. Further work is needed to understand the origin of this difference of sign between HS and the rest of the systems. Thus, in the case of HS, the value of γ increases as the radius of the solid phase becomes smaller. That was already noticed by Auer and Frenkel,[13] Filion *et al.*,[15] and Sharma and Escobedo.[76] However, in the case of the LJ and water models, it is the opposite, the value of γ decreases as the radius of the solid phase becomes smaller. It is also obvious from the previous discussion that using the capillarity approximation (i.e., assuming that the value of the Tolman length is zero or in other words replacing γ_{CNT} by γ_0) in nucleation, studies will yield extremely poor predictions for the nucleation rate. The argument also goes the other way around. Values of γ_{CNT} obtained from fits (using expressions of CNT) to experimental measurements of the nucleation rate cannot be used to estimate the value of the interfacial free energy for the planar interface at coexistence γ_0. Note that although determining experimentally the interfacial free energy for a planar interface at coexistence is quite simple in the case of a vapor-liquid interface, it is extremely difficult from a technical point of view for a solid-liquid interface. For instance, the experimental values (at low pressures) of the interfacial free energy for the ice Ih-water interface at coexistence[77–79] range from the value of 25–35 mJ/m^2. This explains why it has been a common approach to estimate γ_0 for the liquid-solid interface using nucleation studies combined with CNT. This work shows that this approach is wrong.

Let us now discuss the variations of $\gamma_{0,p}$ and δ_p with pressure. As can be seen in Table II, the values of $\gamma_{0,p}$ increase with pressure both for the LJ system[56] and for water.[54] It remains to be explored if this is a general feature in liquid-solid interfaces. Our results suggest that δ_p increases slightly with pressure (nevertheless, the differences are only slightly larger than our statistical uncertainty). Therefore, assuming that δ_p is constant for a certain potential model seems to be a reasonable approximation. If this is the case, the knowledge of the value of δ_p for a given model allows for a relatively simple path to evaluate J over a wide range of temperatures and pressures as will be described in Sec. III.

III. A WORKED EXAMPLE: NUCLEATION OF THE LJ SYSTEM

The combination of Eq. (7) and classical nucleation theory opens up a route to determine J in a relatively easy way. All what is needed are values of γ_0 along the coexistence line (which must also be determined in advance), the value of δ_p for the potential model (we shall assume that is constant and does not change with pressure) and some other magnitudes that can be obtained from simple NpT simulations such as the density of the solid ρ_{sol}, the density of the liquid ρ_{liq}, and $\Delta\mu$, which can be obtained by using thermodynamic integration starting at the coexistence line. The procedure goes as follows:

- Simulations are performed to determine the coexistence line of the model. For instance, direct coexistence simulations can be useful for that purpose, although certainly other routes as free energy calculations are also possible.
- Simulations are performed (using any of the different methods proposed in the literature[4,63,65,68,71,80–83]) to determine the interfacial free energy at coexistence at the pressure of interest for the planar interface for several planes in order to estimate $\gamma_{0,p}$.
- NpT simulations are performed for the liquid and solid phase to determine the equation of state and chemical potentials (via thermodynamic integration from the coexistence point) of both phases.
- Several seeding runs are performed for a certain isobar in the region of interest to determine several values of γ_{CNT} and the value of δ_p. We shall assume that δ_p is hardly affected by pressure and therefore can be used as a constant for a certain potential model.
- At the pressure and temperature of interest, the difference in the chemical potential of both bulk phases $\Delta\mu$ is determined and the value of R_c is obtained by solving the second order equation,

$$R_c = \frac{2\gamma_{CNT}}{(\rho_{sol}\Delta\mu)} = \frac{2\gamma_{0,p}}{(\rho_{sol}\Delta\mu)}\left(1 - \frac{2\delta_p}{R_c}\right). \tag{8}$$

- Once the value of R_c is computed, the value of N_c is obtained as $N_c = \rho_s 4\pi R_c^3/3$, the value of ΔG_c is obtained from Eqs. (4) and (7), and Z is estimated as given by the term under the square root of Eq. (2) (i.e., by the expressions of CNT).
- The attachment rate f^+ is then computed from simulations or alternatively estimated (quite accurately) by using the approximate expression $f^+ = 24D(N_c)^{(2/3)}/\lambda^2$ which relates f^+ to the diffusion coefficient of the metastable liquid D and assuming that the attachment length λ is of the order of a molecular diameter σ as shown in Ref. 33. Thus, from NpT simulations of the metastable liquid, one can determine D and therefore f^+ using the approximate expression.

In summary, knowing the value of δ_p of a certain system allows one to estimate values of J rather easily using information obtained from simple NpT simulations. We shall apply this protocol to the LJ model for four different pressures. The values of γ_0 come from the work of Laird *et al.*[56] These values are presented (along with the values of p and T along the coexistence line of the LJ system) in Table III.

Regarding δ_p, we shall use the value $\delta_p = 0.2425\sigma$ which is close to the average of the two values presented in Table II. We shall assume that δ_p is constant and does not depend on pressure which as discussed above is a good approximation. It is certainly true that

TABLE III. Values of γ_0 along the coexistence line of the LJ systems as reported in Ref. 56. The values of pressure and temperature of the coexistence line are also shown.

$p_m/(\epsilon/\sigma^3)$	$T_m/(\epsilon/k)$	$\gamma_0/(\epsilon/\sigma^2)$
0.00	0.618	0.358
2.29	0.809	0.445
4.95	1.000	0.544
8.74	1.250	0.685

TABLE IV. Values of J for the LJ system alongside their thermodynamic conditions as obtained from brute force simulations.

$p/(\epsilon/\sigma^3)$	$T/(\epsilon/k)$	$\log_{10}(J\sigma^3\tau)$
0.00	0.448	−7.53
2.29	0.579	−7.94
4.95	0.710	−7.84
8.74	0.890	−8.82

seeding runs are still needed to determine the value of δ_p for a certain pressure. However, the procedure outlined here avoids performing seeding runs at other pressures allowing for a relatively fast determination of J over a wide range of temperatures and pressures. In Fig. 4, we show the results of J obtained from the theoretical route of this work (by using a constant value of δ_p). These are compared with results obtained from seeding[28,84] and also from brute force calculations both from this work and from that of Baidakov and Tipeev[85] The values of J from the brute force simulations of this work were obtained from 10 independent NpT runs of a system containing $N = 13\,500$ LJ particles. The value of J was determined as usual from the following expression:

$$J = \frac{1}{\langle t \rangle V}, \tag{9}$$

where $\langle t \rangle$ is the average time for crystallization of the 10 runs. Values of J from the brute force simulations are reported in Table IV.

As can be seen, the agreement between the results of this work and the brute force simulations is quite good. An interesting exercise is to evaluate the effect of δ_p. In Fig. 5, J is presented for $p^* = 0.00$ using $\delta_p = 0.2425\sigma$ and neglecting changes in the interfacial free energy with curvature (i.e., $\delta_p = 0.0\sigma$). As can be seen when using the capillarity approximation, the values of J are too low when compared to the simulation results from brute force simulations. Thus, as reported many times, one cannot use the value of $\gamma_{0,p}$ to obtain γ for nucleation studies.

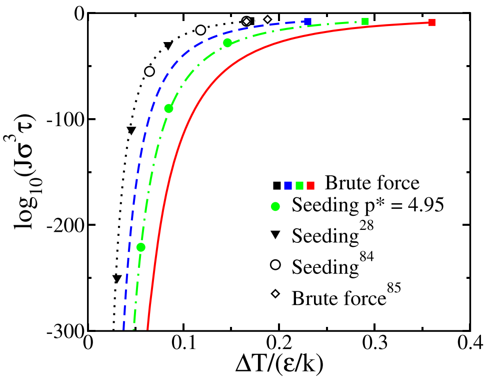

FIG. 4. Nucleation rates J of the LJ system as estimated from the procedure described in the main text for four different isobars (lines) plotted as a function of the supercooling $\Delta T = T_m - T$. From left to right, the results correspond to $p^* = 0.00$, 2.29, 4.95, 8.74. Results from brute force calculations of this work, and from seeding calculations from previous work (for $p^* = 0.00$) and from this work (for $p^* = 4.95$) are also shown.

Let us finish with an interesting exercise. It is relatively straightforward to determine the homogeneous nucleation line T_{HNL}. For each pressure, there is a temperature below which it is not possible to have the metastable liquid because the system freezes. By connecting these temperatures, one obtains the T_{HNL} line. Since the T_{HNL} is a kinetic limit, it depends on the system size and on the typical window time available (which is quite different in simulations and in experiments). In experiments with real substances, $T_{HNL,exp}$ corresponds approximately to the states at which $J = 10^{16}/(\text{m}^3\text{s})$, whereas in simulations of real substances the $T_{HNL,sim}$ corresponds to $J = 10^{30}/(\text{m}^3\text{s})$ as described in detail in previous work.[33] By using the values of $\sigma = 0.3405$ nm and $\epsilon = 0.997$ kJ/mol for argon, we can estimate T_{HNL}. The results are shown in Fig. 6.

As can be seen, the T_{HNL} is not parallel to the melting curve. The distance between the T_{HNL} and the melting line increases with pressure. The important physical conclusion of that is the following: it is more difficult to freeze a supercooled liquid at high pressure. This conclusion could already be anticipated from Fig. 4 where even in brute force simulations we needed further supercooling to obtain spontaneous freezing in the brute force runs. In a recent paper, a similar conclusion was obtained by analyzing the freezing of water under pressure.[54] Thus, the fact that freezing is more difficult under pressure seems to be a general conclusion. Since the value of δ_p does not change much with pressure, the reason behind this behavior is the fact that γ_0 increases with pressure along the coexistence curve

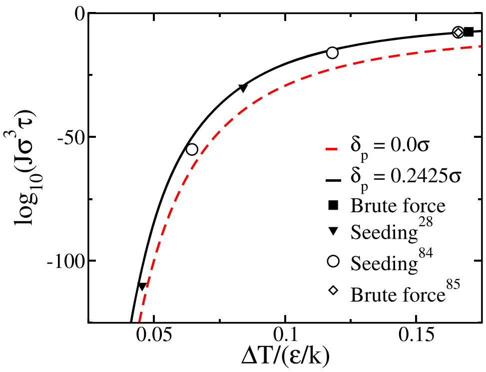

FIG. 5. Nucleation rate J at $p^* = 0.00$ for the LJ model as a function of the supercooling ΔT computed with and without the capillarity approximation. Results are compared to results from brute force calculations and from seeding.

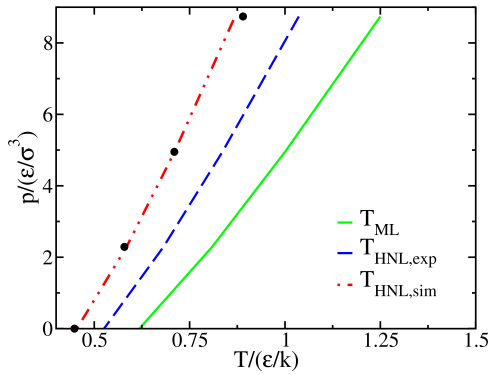

FIG. 6. Temperature at which the homogeneous nucleation is found in experiments $T_{HNL,exp}$ (blue) and in simulations $T_{HNL,sim}$ (red). The melting line of the model (green) is also shown. Solid circles come from the brute force calculations of this work.

both for LJ and for water. We note that the increase in γ_0 with pressure for the Lennard-Jones system is consistent with the empirical proportionality between melting temperature and γ_0 found in close-packed metals.[86] Of course, this rule does not apply to water since γ_0 also increases with pressure despite the fact that the slope of the melting line is negative. In summary, pressure slows down nucleation via an increase in γ_0 both in water and in LJ. Let us discuss now the effect of pressure on nucleation via the diffusion coefficient. In general (water being an exception), the diffusion coefficient of liquids decreases with pressure affecting the attachment rate and so lowering the nucleation rate. Nevertheless, the impact of this kinetic effect on J is rather small as compared to the impact of γ which enters to the third power in the exponential term of Eq. (1) through ΔG_c as reflected by Eq. (4).

To sum up, pressure prevents nucleation in two quite different systems: LJ and water. Although the LJ system has been studied for quite a long time, this conclusion has not been reported (as far as we know) before. Whether this is a general feature of molecular solids, whether other systems also behave in a similar way remains unexplored. Here, by using the simple approach proposed in this work, it is shown that from Ar to water, pressure prevents freezing. The key is γ_0 and now simulations are helping to determine this quantity (which is quite difficult to be obtained experimentally) and to clarify the kinetics of freezing.

IV. CONCLUSIONS

In this paper, the values of the interfacial free energy obtained from seeding studies of nucleation are plotted as a function of $1/R_c$ (including an estimate of the value for $1/R_c = 0$). The plot is linear suggesting that γ can be expanded in series of $1/R_c$ truncated at first order. This is in line with an equation proposed by Tolman 70 years ago.[35] The value of the slope is just given by $-2\gamma_0\delta$, where δ has units of length. We note that the value of γ_0 (i.e., the value of γ for a planar interface under coexistence) can be obtained along isotherms or isobars [or actually through other paths connecting the state of interest (T, p) with the coexistence line]. This leads to two different values of δ, one when γ_0 is obtained under coexistence conditions at the same pressure δ_p and another one when γ_0 is obtained under coexistence conditions at the same temperature δ_T. For freezing studies, it seems to be easier to consider for γ_0 that of coexistence at the same pressure as the system under consideration. The values of δ_p obtained in this work are smaller than a molecular diameter and are positive for LJ, and models of water (mW and TIP4P/ICE) and negative (δ_T) for HS. Their absolute values decrease in the following order: water, HS, and LJ. It is clear from this work that the capillarity approximation (i.e., to neglect curvature effects) cannot be used in nucleation studies. Conversely, if the interfacial free energy is obtained from experimental nucleation studies, the obtained value cannot be taken as an estimate of the equilibrium coexistence value for the planar interface. We have found that the value of δ_p increases slightly with pressure for the LJ and water models. The change is small, and assuming that is constant and does not change with pressure seems to be a good approximation. This allows one to estimate nucleation rates within the CNT formalism (but with magnitudes estimated from computer simulations). For the LJ system, we were able to obtain values of J for four isobars from simple NpT simulations. We also show evidence that the distance from the melting temperature to the homogeneous nucleation line increases with pressure for a LJ system. The same was found previously for water. Thus, pressure might make the formation of solids more difficult for systems as far apart as Ar and water. We hope the approach shown here may be useful in future studies, and we can obtain further molecular understanding on the sign and value of δ both along isotherms (as in the Tolman derivation) and isobars. We have restricted our investigation to the liquid-solid interface. It remains to be studied if the conclusions of this work can or cannot be generalized to the case of the vapor liquid interface. In this work, we have shown that the equation proposed by Tolman in 1949 (although interpreted in a somewhat different way) allows us to understand the nucleation of a number of systems 70 years later.

ACKNOWLEDGMENTS

This work was funded by Grant No. FIS2016-78117-P of the MEC and by Project No. UCM-GR17-910570 from UCM. P.M.d.H. acknowledges financial support from the FPI (Grant No. BES-2017-080074). J.R.E. acknowledges funding and support from the Oppenheimer Research Fellowship and the Emmanuel College Research Fellowship.

REFERENCES

[1] K. F. Kelton and A. L. Greer, *Nucleation in Condensed Matter* (Pergamon, Elsevier, Oxford, 2010).

[2] J. S. Rowlinson and B. Widom, *Molecular Theory of Capillarity* (Oxford University Press, 1982).

[3] B. Cheng, G. A. Tribello, and M. Ceriotti, "Solid-liquid interfacial free energy out of equilibrium," Phys. Rev. B **92**, 180102 (2015).

[4] D. Sopu, J. Rogal, and R. Drautz, "Thermodynamic and kinetic solid-liquid interface properties from transition path sampling," J. Chem. Phys. **145**, 244703 (2016).

[5] W. Cantrell and A. Heymsfield, "Production of ice in tropospheric clouds: A review," Bull. Am. Meteorol. Soc. **86**, 795–808 (2005).

[6] G. Petzold and J. M. Aguilera, "Ice morphology: Fundamentals and technological applications in foods," Food Biophys. **4**, 378–396 (2009).

[7] A. Michaelides and K. Morgenstern, "Ice nanoclusters at hydrophobic metal surfaces," Nat. Mater. **6**, 597 (2007).

[8] R. J. Allen, D. Frenkel, and P. R. ten Wolde, "Simulating rare events in equilibrium or nonequilibrium stochastic systems," J. Chem. Phys. **124**, 024102 (2006).

[9] P. G. Bolhuis, D. Chandler, C. Dellago, and P. L. Geissler, "Transition path sampling: Throwing ropes over rough mountain passes, in the dark," Annu. Rev. Phys. Chem. **53**, 291 (2002).

[10] M. Volmer and A. Weber, "Keimbildung in ubersattigten gebilden," Z. Phys. Chem. **119U**, 277 (1926).

[11] R. Becker and W. Doring, Ann. Phys. **416**, 719–752 (1935).

[12] S. Jungblut and C. Dellago, "Pathways to self-organization: Crystallization via nucleation and growth," Eur. Phys. J. E **39**, 77 (2016).

[13] S. Auer and D. Frenkel, "Prediction of absolute crystal-nucleation rate in hard-sphere colloids," Nature **409**, 1020 (2001).

[14] S. Auer and D. Frenkel, "Quantitative prediction of crystal-nucleation rates for spherical colloids: A computational approach," Annu. Rev. Phys. Chem. **55**, 333 (2004).

[15] L. Filion, M. Hermes, R. Ni, and M. Dijkstra, "Crystal nucleation of hard spheres using molecular dynamics, umbrella sampling, and forward flux sampling: A comparison of simulation techniques," J. Chem. Phys. **133**, 244115 (2010).

[16] L. Filion, R. Ni, D. Frenkel, and M. Dijkstra, "Simulation of nucleation in almost hard-sphere colloids: The discrepancy between experiment and simulation persists," J. Chem. Phys. **134**, 134901 (2011).

[17] S. Prestipino, "The barrier to ice nucleation in monatomic water," J. Chem. Phys. **148**, 124505 (2018).

[18] A. Reinhardt and J. P. K. Doye, "Free energy landscapes for homogeneous nucleation of ice for a monatomic water model," J. Chem. Phys. **136**, 054501 (2012).

[19] G. M. Torrie and J. P. Valleau, "Nonphysical sampling distributions in Monte Carlo free-energy estimation: Umbrella sampling," J. Comput. Phys. **23**, 187–199 (1977).

[20] A. Laio and M. Parrinello, "Escaping free-energy minima," Proc. Natl. Acad. Sci. U. S. A. **99**, 12562 (2002).

[21] H. Niu, Y. I. Yang, and M. Parrinello, "Temperature dependence of homogeneous nucleation in ice," Phys. Rev. Lett. **122**, 245501 (2019).

[22] V. Molinero and E. B. Moore, "Water modeled as an intermediate element between carbon and silicon," J. Phys. Chem. B **113**, 4008–4016 (2009).

[23] X.-M. Bai and M. Li, "Calculation of solid-liquid interfacial free energy: A classical nucleation theory based approach," J. Chem. Phys. **124**, 124707 (2006).

[24] R. G. Pereyra, I. Szleifer, and M. A. Carignano, "Temperature dependence of ice critical nucleus size," J. Chem. Phys. **135**, 034508 (2011).

[25] B. C. Knott, V. Molinero, M. F. Doherty, and B. Peters, "Homogeneous nucleation of methane hydrates: Unrealistic under realistic conditions," J. Am. Chem. Soc. **134**, 19544–19547 (2012).

[26] E. Sanz, C. Vega, J. R. Espinosa, R. Caballero-Bernal, J. L. F. Abascal, and C. Valeriani, "Homogeneous ice nucleation at moderate supercooling from molecular simulation," J. Am. Chem. Soc. **135**, 15008–15017 (2013).

[27] J. R. Espinosa, C. Vega, C. Valeriani, and E. Sanz, "The crystal-fluid interfacial free energy and nucleation rate of NaCl from different simulation methods," J. Chem. Phys. **142**, 194709 (2015).

[28] J. R. Espinosa, C. Vega, C. Valeriani, and E. Sanz, "Seeding approach to crystal nucleation," J. Chem. Phys. **144**, 034501 (2016).

[29] Y. Sun, H. Song, F. Zhang, L. Yang, Z. Ye, M. I. Mendelev, C. Wang, and K. Ho, "Overcoming the time limitation in molecular dynamics simulation of crystal nucleation: A persistent-embryo approach," Phys. Rev. Lett. **120**, 085703 (2018).

[30] D. Kashchiev, *Nucleation: Basic Theory with Applications* (Butterworth-Heinemann, Oxford, 2000).

[31] N. E. Zimmermann, B. Vorselaars, J. R. Espinosa, D. Quigley, W. R. Smith, E. Sanz, C. Vega, and B. Peters, "Nacl nucleation from brine in seeded simulations: Sources of uncertainty in rate estimates," J. Chem. Phys. **148**, 222838 (2018).

[32] W. Lechner and C. Dellago, "Accurate determination of crystal structures based on averaged local bond order parameters," J. Chem. Phys. **129**, 114707 (2008).

[33] J. R. Espinosa, E. Sanz, C. Valeriani, and C. Vega, "Homogeneous ice nucleation evaluated for several water models," J. Chem. Phys. **141**, 18C529 (2014).

[34] A. Zaragoza, M. M. Conde, J. R. Espinosa, C. Valeriani, C. Vega, and E. Sanz, "Competition between ices Ih and Ic in homogeneous water freezing," J. Chem. Phys. **143**, 134504 (2015).

[35] R. C. Tolman, "The effect of droplet size on surface tension," J. Chem. Phys. **17**, 333–337 (1949).

[36] A. Tröster, M. Oettel, B. Block, P. Virnau, and K. Binder, "Numerical approaches to determine the interface tension of curved interfaces from free energy calculations," J. Chem. Phys. **136**, 064709 (2012).

[37] A. Statt, P. Virnau, and K. Binder, "Finite-size effects on liquid-solid phase coexistence and the estimation of crystal nucleation barriers," Phys. Rev. Lett. **114**, 026101 (2015).

[38] E. M. Blokhuis and J. Kuipers, "Thermodynamic expressions for the Tolman length," J. Chem. Phys. **124**, 074701 (2006).

[39] B. J. Block, S. K. Das, M. Oettel, P. Virnau, and K. Binder, "Curvature dependence of surface free energy of liquid drops and bubbles: A simulation study," J. Chem. Phys. **133**, 154702 (2010).

[40] J. G. Sampayo, A. Malijevsky, E. A. Muller, E. de Miguel, and G. Jackson, "Evidence for the role of fluctuations in the thermodynamics of nanoscale drops and the implications in computations of the surface tension," J. Chem. Phys. **132**, 141101 (2010).

[41] A. Malijevsky and G. Jackson, "A perspective on the interfacial properties of nanoscopic liquid drops," J. Phys.: Condens. Matter **24**, 464121 (2012).

[42] H. M. Lu and Q. Jiang, "Size-dependent surface tension and Tolman's length of droplets," Langmuir **21**, 779–781 (2005).

[43] S. Thompson, K. Gubbins, J. Walton, R. Chantry, and J. Rowlinson, "A molecular dynamics study of liquid drops," J. Chem. Phys. **81**, 530–542 (1984).

[44] B. Cheng and M. Ceriotti, "Communication: Computing the Tolman length for solid-liquid interfaces," J. Chem. Phys. **148**, 231102 (2018).

[45] G. V. Lau, I. J. Ford, P. A. Hunt, E. A. Müller, and G. Jackson, "Surface thermodynamics of planar, cylindrical, and spherical vapour-liquid interfaces of water," J. Chem. Phys. **142**, 114701 (2015).

[46] J. Vrabec, G. K. Kedia, G. Fuchs, and H. Hasse, "Comprehensive study of the vapour–liquid coexistence of the truncated and shifted Lennard–Jones fluid including planar and spherical interface properties," Mol. Phys. **104**, 1509 (2006).

[47] O. Wilhelmsen, D. Bedeaux, and D. Reguera, "Tolman length and rigidity constants of the Lennard-Jones fluid," J. Chem. Phys. **142**, 064706 (2015).

[48] M. N. Joswiak, R. Do, M. F. Doherty, and B. Peters, "Energetic and entropic components of the Tolman length for mW and TIP4P/2005 water nanodroplets," J. Chem. Phys. **145**, 204703 (2016).

[49] J. W. P. Schmelzer, A. S. Abyzov, and V. G. Baidakov, "Entropy and the Tolman parameter in nucleation theory," Entropy **21**, 670 (2019).

[50] D. Richard and T. Speck, "Crystallization of hard spheres revisited. II. Thermodynamic modeling, nucleation work, and the surface of tension," J. Chem. Phys. **148**, 224102 (2018).

[51] K. Gunawardana and X. Song, "Theoretical prediction of crystallization kinetics of a supercooled Lennard-Jones fluid," J. Chem. Phys. **148**, 204506 (2018).

[52] A. O. Tipeev, "Comment on "Theoretical prediction of crystallization kinetics of a supercooled Lennard-Jones fluid" [J. Chem. Phys. 148, 204506 (2018)]," J. Chem. Phys. **151**, 017101 (2019).

[53] K. Gunawardana and X. Song, "Response to "Comment on 'Theoretical prediction of crystallization kinetics of a supercooled Lennard-Jones fluid [J. Chem. Phys. 151, 017101 (2019)]'"," J. Chem. Phys. **151**, 017102 (2019).

[54] J. R. Espinosa, A. Zaragoza, P. Rosales-Pelaez, C. Navarro, C. Valeriani, C. Vega, and E. Sanz, "Interfacial free energy as the key to the pressure-induced deceleration of ice nucleation," Phys. Rev. Lett. **117**, 135702 (2016).

[55] J. Russo, F. Romano, and H. Tanaka, "New metastable form of ice and its role in the homogeneous crystallization of water," Nat. Mater. **13**, 733 (2014).

[56] B. B. Laird, R. L. Davidchack, Y. Yang, and M. Asta, "Determination of the solid-liquid interfacial free energy along a coexistence line by Gibbs–Cahn integration," J. Chem. Phys. **131**, 114110 (2009).

[57] J. R. Errington, "Direct calculation of liquid–vapor phase equilibria from transition matrix Monte Carlo simulation," J. Chem. Phys. **118**, 9915–9925 (2003).

[58] J. Broughton and G. Gilmer, "Surface free energy and stress of a Lennard-Jones crystal," Acta Metall. **31**, 845–851 (1983).

[59] J. Jover, A. Haslam, A. Galindo, G. Jackson, and E. Müller, "Pseudo hard-sphere potential for use in continuous molecular-dynamics simulation of spherical and chain molecules," J. Chem. Phys. **137**, 144505 (2012).

[60] J. L. F. Abascal, E. Sanz, R. G. Fernandez, and C. Vega, "A potential model for the study of ices and amorphous water: TIP4P/Ice," J. Chem. Phys. **122**, 234511 (2005).

[61] J. R. Espinosa, C. Navarro, E. Sanz, C. Valeriani, and C. Vega, "On the time required to freeze water," J. Chem. Phys. **145**, 211922 (2016).

[62] J. R. Espinosa, C. Vega, and E. Sanz, "Ice-water interfacial free energy for the TIP4P, TIP4P/2005, TIP4P/ice and mW models as obtained from the mold integration technique," J. Phys. Chem. C **120**, 8068–8075 (2016).

[63] R. L. Davidchack, J. R. Morris, and B. B. Laird, "The anisotropic hard-sphere crystal-melt interfacial free energy from fluctuations," J. Chem. Phys. **125**, 094710 (2006).

[64] J. R. Morris and X. Song, "The anisotropic free energy of the Lennard-Jones crystal-melt interface," J. Chem. Phys. **119**, 3920–3925 (2003).

[65] J. J. Hoyt, M. Asta, and A. Karma, "Method for computing the anisotropy of the solid-liquid interfacial free energy," Phys. Rev. Lett. **86**, 5530–5533 (2001).

[66] R. Handel, R. L. Davidchack, J. Anwar, and A. Brukhno, "Direct calculation of solid-liquid interfacial free energy for molecular systems: TIP4P ice-water interface," Phys. Rev. Lett. **100**, 036104 (2008).

[67] L.-K. Wu, Q.-L. Li, M. Li, B. Xu, W. Liu, P. Zhao, and B.-Z. Bai, "Calculation of solid–liquid interfacial free energy and its anisotropy in undercooled system," Rare Met. **37**, 543 (2018).

[68] J. R. Espinosa, C. Vega, and E. Sanz, "The mold integration method for the calculation of the crystal-fluid interfacial free energy from simulations," J. Chem. Phys. **141**, 134709 (2014).

[69] R. L. Davidchack and B. B. Laird, "Crystal structure and interaction dependence of the crystal-melt interfacial free energy," Phys. Rev. Lett. **94**, 086102 (2005).

[70] R. L. Davidchack, "Hard spheres revisited: Accurate calculation of the solid–liquid interfacial free energy," J. Chem. Phys. **133**, 234701 (2010).

[71] E. Baldi, M. Ceriotti, and G. A. Tribello, "Extracting the interfacial free energy and anisotropy from a smooth fluctuating dividing surface," J. Phys.: Condens. Matter **29**, 445001 (2017).

[72] P. Koß, A. Statt, P. Virnau, and K. Binder, "Free-energy barriers for crystal nucleation from fluid phases," Phys. Rev. E **96**, 042609 (2017).

[73] P. Koß, A. Statt, P. Virnau, and K. Binder, "The phase coexistence method to obtain surface free energies and nucleation barriers: A brief review," Mol. Phys. **116**, 2977–2986 (2018).

[74] N. Bruot and F. Caupin, "Curvature dependence of the liquid-vapor surface tension beyond the Tolman approximation," Phys. Rev. Lett. **116**, 056102 (2016).

[75] S. Kim, D. Kim, J. Kim, S. An, and W. Jhe, "Direct evidence for curvature-dependent surface tension in capillary condensation: Kelvin equation at molecular scale," Phys. Rev. X **8**, 041046 (2018).

[76] A. K. Sharma and F. A. Escobedo, "Nucleus-size pinning for determination of nucleation free-energy barriers and nucleus geometry," J. Chem. Phys. **148**, 184104 (2018).

[77] L. Granasy, T. Pusztai, and P. F. James, "Interfacial properties deduced from nucleation experiments: A Cahn–Hilliard analysis," J. Chem. Phys. **117**, 6157–6168 (2002).

[78] H. R. Pruppacher, "A new look at homogeneous ice nucleation in supercooled water drops," J. Atmos. Sci. **52**, 1924 (1995).

[79] S. Hardy, "A grain boundary groove measurement of the surface tension between ice and water," Philos. Mag. **35**, 471–484 (1977).

[80] J. Q. Broughton and G. H. Gilmer, "Molecular dynamics investigation of the crystal–fluid interface. VI. Excess surface free energies of crystal–liquid systems," J. Chem. Phys. **84**, 5759–5768 (1986).

[81] S. Angioletti-Uberti, M. Ceriotti, P. D. Lee, and M. W. Finnis, "Solid-liquid interface free energy through metadynamics simulations," Phys. Rev. B **81**, 125416 (2010).

[82] L. A. Fernandez, V. Martin-Mayor, B. Seoane, and P. Verrocchio, "Equilibrium fluid-solid coexistence of hard spheres," Phys. Rev. Lett. **108**, 165701 (2012).

[83] R. Benjamin and J. Horbach, "Crystal-liquid interfacial free energy via thermodynamic integration," J. Chem. Phys. **141**, 044715 (2014).

[84] A. O. Tipeev, E. D. Zanotto, and J. P. Rino, "Diffusivity, interfacial free energy, and crystal nucleation in a supercooled Lennard-Jones liquid," J. Phys. Chem. C **122**, 28884–28894 (2018).

[85] V. G. Baidakov and A. O. Tipeev, "Crystal nucleation and the solid–liquid interfacial free energy," J. Chem. Phys. **136**, 074510 (2012).

[86] B. B. Laird, "The solid–liquid interfacial free energy of close-packed metals: Hard-spheres and the turnbull coefficient," J. Chem. Phys. **115**, 2887–2888 (2001).